Modeling the Resolution for Photoacoustic Bio-Microscopy in the Giga-Hertz Frequency Range

Chukwunomso Agunwamba

Mathematics and Physics, Worcester Polytechnic Institute

NNIN REU Site: Center for Nanoscale Systems, Harvard University

NNIN REU Principal Investigator: Shriram Ramanathan, School of Engineering and Applied Sciences, Harvard University

Contact: nomnso@wpi.edu, shriram@seas.harvard.edu

Abstract

Photoacoustic (PA) methods promise higher image resolution with an increase in the acoustic wave's frequency. However, they are effectively limited by the wave's penetration depth as the frequency enters the gigahertz range [1,2]. In this project, we explored the relationship between depth, initial center frequency, and amplitude for the acoustic pulse. First, arrangements of transducers and metallic particles were specified for the PA microscope. For the setup, a discrete time model was used to show how to obtain an image, to develop relations both for the resolution. This model was simulated in MATLAB®.

Introduction

Previously, in a paper [3] by Daniel Wulin and Shriram Ramanathan, curves relating the center acoustic frequency for metallic and silica particles to their radii were generated and discussed. For a fluid, they also showed how the initial center frequency of a Gaussian acoustic pulse is downshifted as a function of depth traveled. This project proposes several transducer and metallic particle arrangements for a PA bio-microscope. It can be useful for non-invasive examination of the structure of biological media and molecules (such as fat) and individual cells or tissues. It uses acoustic waves generated from the elastic response of nano-sized metallic particles to a laser pulse train. The lateral and axial resolutions from the resulting image are modeled in terms of the maximum center frequency allowed by selected biological media and the acoustic pulse's bandwidth.

Theory

The acoustic pulse, *h(m)*, would pass through a sequence of interfaces while experiencing reflections represented as r_k, transmission represented as $(1\text{-}r_k)$, and attenuation between interfaces represented as $\alpha(\omega l)$. The absorption coefficient is a function of the center frequency. Its expression depends on the medium. In the MHz range, this curve has been determined for several biological media. For example, attenuation coefficient for water is known to have an f^2 relationship with frequency in the MHz range [4]. It is assumed that the signal containing reflected-acoustic pulses and the signal containing emitted-acoustic pulses are spatially and temporally sampled once they are received.

The signal coming from the imaged sample is a superposition of scaled and delayed pulses that have the same profile as the original emitted pulse. It is assumed that there is weak temporal dispersion of the composite acoustic pulse formed by the superposition of several center frequencies, ω_l. The de-convolved spectrum is, therefore, a linear combination of scaled and delayed sinusoidal functions in the frequency domain. $S(\omega)$ is the impulse response of the transducer, while $H(\omega,\omega_l)$ is the spectrum of Gaussian acoustic pulse with a center frequency of ω_l. The spectrum, $X(\omega,\omega_l)$, contains the information about attenuation, reflection, and the time delay for each echo pulse in the signal.

The axial resolution [5,6] is treated as being quite independent of the center frequency. The stress and thermal confinements of the laser pulse temporal width is given by t_s and t_{th} [7]. This, in turn, limits the temporal width of the acoustic pulse it modulates. V_o is the velocity of the acoustic pulse in the medium housing the metallic particles and the transducers. V_j is in the space after the *jth* interface. To calculate depth, the velocity of the acoustic pulse is assumed constant within the imaged medium, only depending on the center frequency. It is also assumed that the medium housing the metallic particles and the transducers has an impedance matching the imaged sample.

The lateral resolution is obtained using the diameter of the transducer, d_t, its focal length, the maximum center frequency, $\omega_{l_{att}}$. The frequency, $\omega_{l_{att}}$, is the highest frequency with the minimum detectable intensity in the signal.

$$Y(\omega) = S(\omega)\sum_{l} X(\omega,\omega_l)H(\omega,\omega_l),\ X(\omega) = \sum_{k=1}^{J} C_k(\omega_l)e^{-i\tau(k,\omega_l)\omega},$$

$$H(\omega,\omega_l) = \left(\frac{I_O}{\sigma_l\sqrt{2\pi}}\right)\left[e^{-(\omega-\omega_l)^2/(2\sigma_l^2)}\right].$$

$$C_k^2(\omega_l) = C_{k-1}^2(\omega_l)\times\left[e^{-(\alpha(\omega_l)Y(\omega_l)\times\Delta t_k(\omega_l))}\right]\left[(1-r_{k-1})^2\right](r_k)/(r_{k-1})$$

Here, $\omega = 2\pi\frac{k}{F_s}$, k is frequency in Hz, and F_s is the sampling frequency in Hz satisfying the Nyquist rate.

$$\text{Single Transducer Axial resolution} = R_A = \frac{V_O}{2\times FWHM\left(\left|S(\omega)\sum_{l} H(\omega,\omega_l)X(\omega,\omega_l)\right|\right)} \geq t_a\times\min(V_j)/2$$

Here, the initial acoustic pulse temporal width $= t_a \leq \min(t_s, t_{th})$.

Highest center frequency detected at the transducer after being attenuated by the medium $= \omega_{l_{att}}$

$$\text{Lateral resolution} = R_L \propto \frac{\lambda_O\times\text{focal length}}{d_t} = \frac{2\pi V_O\times\text{focal length}}{\omega_{l_{att}}\times d_t}$$

The depth profile is resolved with time, under the assumption of a linear relationship between reflection depth and 'time-of-flight'. Here, the time-of-flight is the time for the wave to travel from the metallic particle(s) to an interface in the sample and to a receiving transducer. The assumption of a linear relationship implies that the wave maintains a constant velocity within each sub-medium of fixed characteristic impedance. The velocity only changes to a new value when the wave enters a region having a different characteristic impedance.

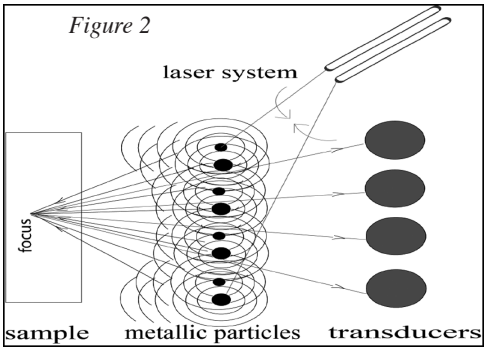

Design

In Figure 2, a single laser beam excited a metallic particle or a cluster of metallic particles. (The black and the blue arrows trace the path of the rays to the transducer.) To direct and focus the beam, the light, from two lasers, swept in the directions indicated by the green arrows. The sweeping can also be done by one laser and a beam splitter. The sweeping action caused a relative time delay and a sequential excitation of the metallic particles. A curved wave front was created, according to Huygens's principle. This idea was adapted from a description in a paper by P. N. T. Wells [8]. There, he describes how the sequential excitation of elements in a transducer array focuses and directs the acoustic wave beam. The difference is that a laser system and metallic particles are used in generating the acoustic wave in this paper.

The pulse-echo method relied on waves that are reflected at interfaces with mismatched acoustic impedances (See Figures 3 and 4). At any such interface, a fraction of the wave was transmitted into the new medium while the other portion was reflected. Each transducer element recorded the amplitude of the acoustic wave that passed by its position.

Conclusion

A discrete pulse-echo model was developed and simulated in MATLAB to explore how the combination of high acoustic frequency, with the transducer setup, density of metallic particles, and choice of center frequencies, can make possible very fine resolutions in the range between micrometer and nanometer scales. Some follow up studies include: modeling how the nanoparticles control and shape the wave fronts in time and space, studying different materials and fluids for housing the nano-particles and the transducer, and making measurements of the attenuation coefficient of biological media in the giga-hertz range.

Acknowledgments

The author acknowledges funding from the NNIN Research Experience for Undergraduates Program through Harvard University for this part of the research.

References

[1] "Photoacoustic imaging in biomedicine" by M. Xu, and L.V. Wang, Rev. Sci. Instrum. 77, 041101 (2006).

[2] "Acoustic Microscopy: Biomedical Applications" by Ross A. Lemons, and Calvin F. Quate, Science, New Series, Vol. 188, No. 4191. (May 30, 1975), pp. 905-911.

[3] "Non-invasive high-resolution acoustic microscopy technique using embedded nanostructures" by Daniel Wulin, and Shriram Ramanathan, Mater. Res. Soc. Symp. Proc. (2007).

[4] "Ultrasonic imaging of the human body" by P N T Wells, Rep. Prog. Phys. 62 (1999) 671-722.

[5] "Advances In Ultrasound Biomicroscopy" by F. Stuart Foster, Charles J. Pavlin, Kasia A. Harasiewicz, Donald A. Christopher, and Daniel H. Turnbull, Ultrasound in Med. & Biol., Vol. 26, No. 1, pp. 1-27, 2000.

[6] "Analytic explanation of spatial resolution related to bandwidth and detector aperture size in thermoacoustic or photoacoustic reconstruction" by Minghua Xu and Lihong V. Wang, Phys. Rev. E 67, 056605 (2003).

[7] "Photoacoustic imaging in biomedicine" by M. Xu, and L.V. Wang, Rev. Sci. Instrum. 77, 041101 (2006).

[8] "Ultrasonic imaging of the human body" by P N T Wells, Rep. Prog. Phys. 62 (1999) 671-722.

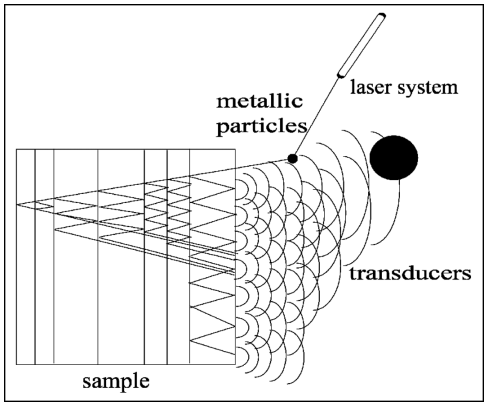

Figure 3: Reflections, transmissions, and absorptions occur each time a ray path meets an interface.

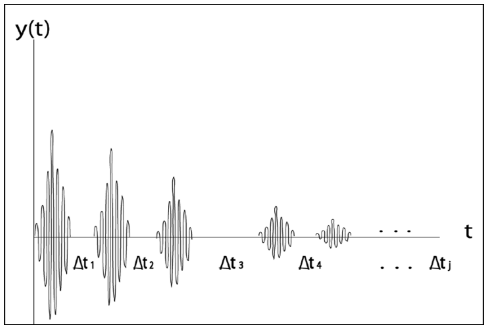

Figure 4: The echo signal as a combination of delayed pulses. The delay depends on the acoustic wave velocity in the sample and the distance between interfaces. These dependencies could cause the echoes to overlap.